
MEGU: MACHINE-GUIDED UNLEARNING WITH TARGET FEATURE DISENTANGLEMENT

A PREPRINT

Haoyu Wang¹, Zhuo Huang², Xiaolong Wang¹, Bo Han³, Zhiwei Lin¹, Tongliang Liu²

¹School of Automation, Beijing Institute of Technology; ²Sydney AI Centre, The University of Sydney;

³Department of Computer Science, Hong Kong Baptist University

ABSTRACT

The growing concern over training data privacy has elevated the "Right to be Forgotten" into a critical requirement, thereby raising the demand for effective Machine Unlearning. However, existing unlearning approaches commonly suffer from a fundamental trade-off: aggressively erasing the influence of target data often degrades model utility on retained data, while conservative strategies leave residual target information intact. In this work, the intrinsic representation properties learned during model pretraining are analyzed. It is demonstrated that semantic class concepts are entangled at the feature-pattern level, sharing associated features while preserving concept-specific discriminative components. This entanglement fundamentally limits the effectiveness of existing unlearning paradigms. Motivated by this insight, we propose Machine-Guided Unlearning (MeGU), a novel framework that guides unlearning through concept-aware re-alignment. Specifically, Multi-modal Large Language Models (MLLMs) are leveraged to explicitly determine re-alignment directions for target samples by assigning semantically meaningful perturbing labels. To improve efficiency, inter-class conceptual similarities estimated by the MLLM are encoded into a lightweight transition matrix. Furthermore, MeGU introduces a positive-negative feature noise pair to explicitly disentangle target concept influence. During finetuning, the negative noise suppresses target-specific feature patterns, while the positive noise reinforces remaining associated features and aligns them with perturbing concepts. This coordinated design enables selective disruption of target-specific representations while preserving shared semantic structures. As a result, MeGU enables controlled and selective forgetting, effectively mitigating both under-unlearning and over-unlearning. Extensive experiments across varying unlearning scenarios and diverse datasets demonstrate that MeGU consistently outperforms state-of-the-art baselines, achieving thorough target data removal while maintaining strong generalization performance on retained data.

1 Introduction

Machine Learning (ML), based on utilization of data resources, has been extensively explored in vast fields [Jordan and Mitchell, 2015, Lu and Weng, 2007, Nadkarni et al., 2011]. However, studies [Jegorova et al., 2022, Fu et al., 2022] highlight the potential data security risks such as differential privacy [Dwork et al., 2014] and adversarial vulnerabilities [Steinhardt et al., 2017]. Regulations [Voigt and Von dem Bussche, 2017, Bonta, 2022] have been introduced to address these concerns, where the "Right to be Forgotten" [Rosen, 2011] is underlined to enable deletion request from data providers to protect their privacy. On the other hand, part of the information exposed to a model during the training phase is often time-sensitive or inherently unreliable, such as noisy labels. Eliminating the influence of such unreliable information on a deployed model without resorting to retraining constitutes another critical requirement for achieving trustworthy AI [Hine et al., 2024, Kang et al., 2025, Huang, 2025, Wang et al., 2024a, Li et al., 2024, Yuan et al., 2024, 2025]. To fulfill this target, an intuitive solution is to train a new model from scratch without target data. However, the substantial computation and time costs are simply unacceptable for practices. Thereby, the Machine Unlearning (MU) is proposed to tackle this problem, whose objectives are: 1) Remove the influence of specific data while maintaining the overall generalization; 2) Cost less time and computational resources than simply retraining.

Prior researchers mainly explore two types of unlearning strategies: model-centric and data-centric approaches. Model-centric methods directly modify model architectures or parameters through alternative training paradigms [Bourtoule et al., 2021, Yan et al., 2022] or influence estimation [Sekhari et al., 2021, Zhao et al., 2022]. While data-centric approaches [Golatkar et al., 2020a, Shibata et al., 2021] utilize re-optimization [Golatkar et al., 2020a] or gradient updates [Wu et al., 2020, Huang et al., 2026] to align the unlearned model with the retrained model, called "gold model". However, these approaches often face problems such as storage overhead and inaccurate unlearning. Another line of works [Graves et al., 2021], such as UNSIR [Tarun et al., 2023], crave to leverage feature noises to enhance forgetting of target data during fine-tuning. However, empirical evidence suggests a trade-off between effectively eliminating the influence of target data and maintaining the overall generalization capability [Ye et al., 2021, Huang et al., 2023, 2025].

To address this challenge, we first investigate in a question: *How does the unlearned data affect the retained model generalization?* Existing research [Serra et al., 2018] indicates that models acquire two levels of cognition during pretraining: **feature patterns** directly extracted from data, and **semantic concepts** representing complex relations and combinations of different feature patterns, during pretraining. Prior study [Chang et al., 2024] interprets it as a mapping of features onto a higher-dimensional concepts space. This explains the interleaved influence that unlearned data poses on the retained model generalization, as different semantic concepts could share certain amounts of patterns, hereby named as associated features, while they each have unique features to distinguish from others. Figure 1 shows such an example. When unlearning one of the concept, the associated features between two concepts are restrained, harnessing the generalization on the retained concept. Such interplay underscores the nature of the trade-off challenge. However, previous studies focus either on eliminating all related feature patterns of target concept [Tarun et al., 2023] or re-aligning the target concept with other retained concepts [Chen et al., 2023]. The complex entanglement at the feature pattern level is neglected, leading to excessive or insufficient unlearning.

In this paper, we propose Machine-Guided Unlearning (MeGU) as a framework to manipulate and enhance the unlearning process, as shown in Figure 2. Intuitively, MeGU aims to unlearn certain data by injecting misleading concepts to ensure learning a desired semantic gap from the target data. To achieve this, we leverage the guidance of zero-shot Multi-modal Large Language Models (MLLMs) [Liu et al., 2024a, Huang et al., 2024] to generate perturbing labels for finetuning. The similarities between different concepts are based on the understanding of prompted MLLMs. We store such a similarity in a transition matrix, which facilitates efficient inference of subsequent instance-based feature understanding. Furthermore, to address the problem of feature entanglement, we introduce the Fragment-Align strategy, which disentangles semantic concepts via a positive-negative feature noise pair Hong et al. [2024, 2022], Chen et al. [2025]. Specifically, the positive feature noise aims to align the target data representation with the semantics of the perturbing labels, while the negative feature noise disrupts the original representation associated with the true labels. Working together, these two complementary noises disentangle the target features from their original concepts and re-anchor them toward the perturbed concepts, enabling selective forgetting without harming overall generalization. Through substantial studies on three unlearning tasks conducted on a range of datasets, the efficacy and efficiency of MeGU as an unlearning method are rigorously validated. Our contributions in this paper can be summarized into:

- We investigate the intrinsic mechanisms underlying model generalization from a two-level cognitive perspective, namely feature patterns and semantic concepts. We further uncover the entangled interactions among different concepts, which give rise to the inherent trade-off challenges faced by existing unlearning approaches.
- We propose MeGU, a novel framework that leverages MLLM guidance to explicitly manipulate the unlearning process. Building upon this framework, we introduce the Fragment-Align strategy to disentangle the influence of target data, thereby effectively alleviating the aforementioned trade-off. Moreover, we provide both theoretical analysis and empirical evidence to systematically differentiate MeGU from representative unlearning paradigms.
- We conduct extensive evaluations across three distinct unlearning scenarios to rigorously assess the effectiveness of the proposed method. In addition, we perform comprehensive ablation and sensitivity studies to examine the

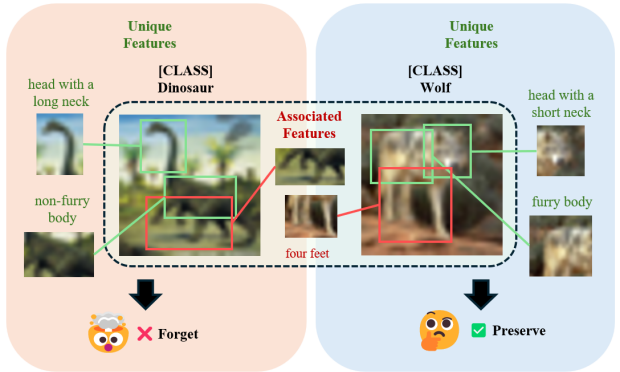


Figure 1: The entanglement among features from different concepts. Taking dinosaur and wolf as an example. They share similar features (marked as red) while each possesses unique features (green). Assume that dinosaur is the class to be forgotten. The goal of our method is to disentangle its features and forget the target concept's unique features while preserving associated features shared with the other retained concepts.

contributions of individual components within the framework as well as the impact of key hyperparameter settings. Detailed analyses of experimental results are presented to substantiate our claims.

2 Related works

2.1 Machine unlearning

Existing Machine Unlearning (MU) approaches can be categorized into two branches: model-centric and data-centric unlearning. Model-centric unlearning endeavors to repurpose knowledge from pre-trained models by selectively modifying or filtering their components or parameters, such as Sharded, Isolated, Sliced, and Aggregated (SISA) training [Bourtoule et al., 2021]. Researchers [Yan et al., 2022, Zhou et al., 2022, Brophy and Lowd, 2021] continue to improve the performance through techniques such as data preprocessing. However, isolated training of model components will lead to generalization degradation and additional costs for initial training and storage. Model pruning [Zhao et al., 2022, Liu et al., 2024b, Wang et al., 2022, Tanaka et al., 2020, Feldman, 2020, Stephenson et al., 2021], emerges to discard target data by selectively manipulating related crucial parameters [Yeom et al., 2021, Ma et al., 2021, Frankle and Carbin, 2018]. Besides, the influence functions are typically approximated to estimate the essence of parameters to target data [Wu et al., 2022, Sekhari et al., 2021, Suriyakumar and Wilson, 2022, Foster et al., 2024, Golatkar et al., 2020a, Yang et al., 2025]. Nevertheless, the risk of over-unlearning persists, as parameters important for forgetting data may also play a significant role for retained data [Chang et al., 2024]. Data-centric unlearning aims to adjust pre-trained models through re-optimization and gradient updates [Neel et al., 2021, Cao et al., 2023, Graves et al., 2021, Shaik et al., 2024, Fan et al., 2023, Wang et al., 2025a,b] to address forgetting requests. [Golatkar et al., 2020a] introduce a scrubbing function during finetuning stage to align the unlearned model with the "gold model", which is continuously refined by subsequent research [Golatkar et al., 2021, 2020b, Shibata et al., 2021, Mehta et al., 2022, Tanno et al., 2022]. DeltaGrad [Wu et al., 2020] and BAERASER [Liu et al., 2022] employ gradient updates using cached weight information during training to unlearn target data. Despite their achievements, methods of this kind rely on strong convexity assumptions, leading to unavoidable approximation errors. Alternative approaches have explored the utilization of feature noise [Tarun et al., 2023, Wang et al., 2024b] and label noise [Chen et al., 2023] to diminish the generalization of forgetting data. Teacher-student framework [Chundawat et al., 2023, Zhang et al., 2023, Lin et al., 2023, Huang et al., 2022] is also employed to selectively distill knowledge, excluding forgetting data. While these methods provide intuitive solutions, they still face the inherent trade-offs problem of excessive or insufficient unlearning.

2.2 In-context Learning of Multi-modal large language models

The emergence of Transformer [Vaswani, 2017] facilitates the development of Large Language Models (LLM) [Brown, 2020, Floridi and Chiratti, 2020, Touvron et al., 2023a,b]. Incorporated with Vision Transformer (ViT) [Dosovitskiy, 2020], LLM is equipped with efficient multi-modal capabilities, known as Multi-modal Large Language Models (MLLM) [Li et al., 2022, 2023, Liu et al., 2024a, Dai et al., 2023, Ye et al., 2023]. By integrating Vision Transformers (ViT) [Dosovitskiy, 2020] and cross-modal alignment modules, LLMs are extended to Multi-modal Large Language Models (MLLMs), enabling joint reasoning over text and visual inputs [Li et al., 2022, 2023, Dai et al., 2023, Ye et al., 2023]. Within this framework, the representations of text and images are aligned through an intermediate structure. In this setting, ICL allows models to perform zero-shot or few-shot task adaptation by conditioning on input demonstrations, without updating model parameters [Brown, 2020]. Studies suggest that ICL can be interpreted as a form of implicit meta-learning or Bayesian inference over latent task structures [Garg et al., 2022, Xie et al., 2021]. Building on this paradigm, MMICL [Zhao et al., 2023a] introduces a context training strategy that interleaves visual embeddings with textual tokens, significantly enhancing multimodal in-context generalization. Related works [Alayrac et al., 2022, Liu et al., 2024a] further indicate that multimodal ICL not only supports task adaptation, but also reveals the internal alignment and similarity structure of learned visual-semantic concepts. These properties make MLLMs a natural tool for probing conceptual relationships across classes. In this paper, we propose to leverage the strengths of MLLMs to guide the unlearning process through a novel perturbing label assigning strategy. The in-context learning capabilities of MLLMs are utilized to estimate the similarities of feature patterns among different class concepts, which subsequently guarantees the disentanglement of influence of target data.

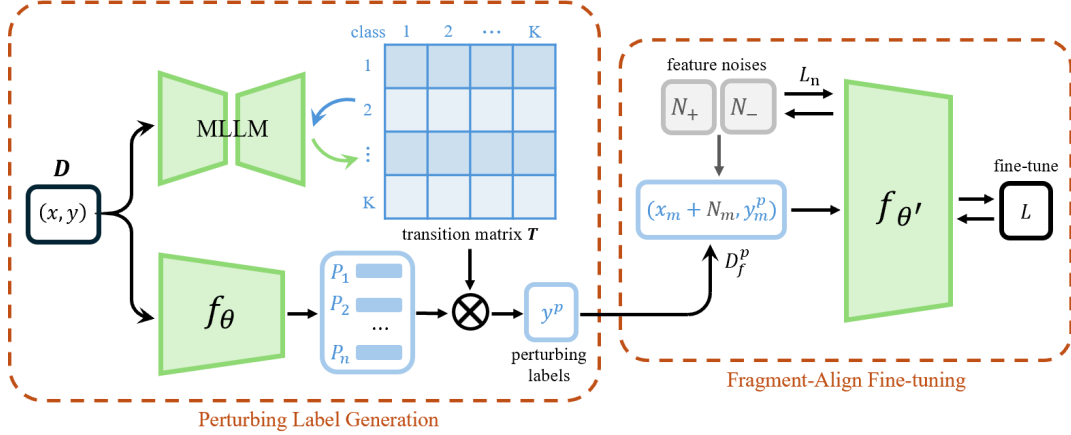


Figure 2: The proposed unlearning framework MeGU. The MLLM is employed to acquire the conceptual similarities with a small subset of the training data. Incorporated with model prediction, the perturbing labels are determined. The Fragment-Align strategy leverages a pair of feature noises trained from the frozen pretrained model to respectively restrain unique features of the target data while enhancing those associated with the retained data. The unlearning is achieved via aligning the target data towards perturbing labels while disentangling their influence.

3 Preliminaries

Problem setup Given a dataset $\mathcal{D} = \{x_i, y_i\}_{i=1}^N$ where y_i belongs to label space $\mathcal{Y} = \{1, \dots, K\}$, the objective of machine learning can be formalized as:

$$\theta = \arg \min_{\theta} \sum_{(x_i, y_i) \in \mathcal{D}} \mathcal{L}(f_{\theta}(x_i), y_i) \quad (1)$$

where f_{θ} is the DNN model parameterized by θ , and \mathcal{L} denotes the training loss function. In the scenario of machine unlearning, the goal is to remove the influence of a designated forget set $\mathcal{D}_f \subset \mathcal{D}$ from the pre-trained model f_{θ} , while preserving its performance on the retain subset $\mathcal{D}_r = \mathcal{D} \setminus \mathcal{D}_f$. This process yields the unlearned model $f_{\theta'}$, where θ' represents the updated parameters.

Building upon prior studies [Alzubaidi et al., 2021, Allen-Zhu and Li, 2023], deep learning models are widely recognized to process and interpret inputs in a hierarchical manner, wherein progressively deeper layers encode increasingly abstract and semantically rich representations. As the network depth increases, model parameters are able to capture more complex feature compositions that correspond to higher-level semantic concepts. Motivated by this perspective, we hypothesize that during pre-training, the model learns a series of feature patterns and their corresponding mappings to semantic concepts. This process can be formalized as $\mathcal{P}_k \mapsto \mathcal{C}_k, k \in [1, K]$, where $\mathcal{P}_k = \{p_{k1}, \dots, p_{kM}\}$ denotes the features of the semantic concept \mathcal{C}_k from class k .

As shown in Figure 1, different concepts may share similar feature patterns, which add to the complexity of the unlearning process. Thereby, we further straighten out such connections among concepts. For two distinct concepts \mathcal{C}_i and \mathcal{C}_j , we define the intersection of their feature patterns $\mathcal{P}_{ij}^{ass} = \mathcal{P}_i \cap \mathcal{P}_j$ as the **associated features**, while the **unique features** of concept \mathcal{C}_i and \mathcal{C}_j are defined as $\mathcal{P}_i^{uni} = \mathcal{P}_i \setminus \mathcal{P}_{ij}^{ass}$ and $\mathcal{P}_j^{uni} = \mathcal{P}_j \setminus \mathcal{P}_{ij}^{ass}$ other than the shared part.

Unlearning via training with error-maximizing noise The previous method, UNSIR, endeavors to achieve unlearning through deliberately inducing catastrophic forgetting about specific target data. This process is achieved through a two-step paradigm:

$$\begin{aligned} \theta'_{impair} &= \arg \min_{\theta'} \sum_{(x_i, y_i) \in \mathcal{D}_r} \mathcal{L}(f_{\theta}(x_i + \mathcal{N}_f), y_i) \\ \theta'_{repair} &= \arg \min_{\theta'} \sum_{(x_i, y_i) \in \mathcal{D}_r} \mathcal{L}(f_{\theta}(x_i), y_i) \end{aligned} \quad (2)$$

where \mathcal{N}_f denotes Error-maximizing noise. It is a matrix of the same size as that of the model input, randomly initialized and then trained from the frozen pretrained model through the process:

$$\mathcal{N}_f = \arg \min_{\mathcal{N}} \mathbb{E}(-\mathcal{L}(f_{\theta}(\mathcal{N}), y_i^p) + \lambda \|\mathcal{N}\|) \quad (3)$$

In this manner, \mathcal{N}_f extracts counteracting feature information that is semantically opposite to the target data from the frozen pretrained model. Under the classification loss \mathcal{L} , these anti-feature representations can induce gradient

update directions that oppose to those driven by the target data. Consequently, during the impair stage in Equation 2, when \mathcal{N}_f is incorporated together with the retain data \mathcal{D}_r and optimized with respect to y_i , the model’s originally well-aligned optimization trajectory for target-related features is deliberately disrupted. As a result, the model’s ability to accurately capture and exploit features associated with the target data is significantly degraded, thereby effectively realizing concept-level forgetting of the target data.

However, this approach does not account for feature entanglement across different semantic concepts. The error-maximizing noise indiscriminately extracts all anti-feature representations associated with the target data. Directly using these representations for model fine-tuning without proper selection or disentanglement risks disrupting the model’s understanding of features relevant to the retained data. Moreover, this strategy operates solely at the level of feature representations. Owing to the absence of explicit manipulation of the target data’s semantic concepts during the unlearning stage, the mapping from feature patterns to the target semantic concept may still persist in the model’s latent space, ultimately resulting in incomplete and insufficient forgetting.

4 Methodology

In this section, we introduce MeGU for effective machine unlearning, which combines two components: 1) the MLLM guided label perturbation and 2) the Fragment-Align strategy. As shown in Figure 2, we first estimate inter-concept similarities using zero-shot MLLMs on a subset of training data, and cache them in a lightweight transition matrix. Further, based on the pretrained model’s predictions, the transition matrix can assign proper label perturbation to achieve manipulation of concepts. For each forgetting instance, the pre-trained and cached feature noises are injected to disentangle their influence. Furthermore, we utilize MLLM guidance to quantify inter-concept distances to ensure effective label perturbation and identification of the class for positive noise, thereby preserving the retained data. In the following sections, we first demonstrate the process to generate perturbing labels in Section 4.1. Then, in Section 4.2, we carefully elucidate the Fragment-Align strategy for influence disentanglement and the fine-tuning method to unlearn target data.

4.1 Perturbing labels generation

Intuitively, to induce model unlearning, MeGU introduces semantically consistent but incorrect labels at the finetuning stage to replace the learned connections of target data to their correct labels with a meaningful but alternative relation to the retained concepts. To achieve this, we leverage MLLM to estimate the semantic consistency among concepts to assign suitable perturbing labels. To reduce the computation costs, we use a light-weight transition matrix to capture inter-concept similarities derived by the MLLM using a small subset from the training data. This matrix, encoding the knowledge of the MLLM, can be repetitively used for perturbing label assignment without further MLLM calls.

Transition matrix estimation Specifically, let q_w be the MLLM model parameterized by w . We randomly select n exemplars from each class in the dataset \mathcal{D} to construct the subset \mathcal{D}_{ex} . Then we prompt the MLLM model q_w to estimate feature similarity of each instance in \mathcal{D}_{ex} to all other semantic concepts. For example, given a query image from class k and its counterpart $l \in [1, K]$, the prompt is:

Question: This image <IMG_l> shows a photo of <label_l>, True or False? Answer: True;
 Question: This image <IMG_p> shows a photo of <label_l>, True or False? Answer: False;
 Question: This image <IMG_k^{query}> shows a photo of <label_l>, True or False? Answer:

In this way, the MLLM output is restricted to binary answers, i.e., True or False. Then, the feature similarity can be represented by softmax output logits.

To compute the feature similarity matrix among concepts, let x_i be an instance from class k in \mathcal{D}_{ex} , and $q_w(\cdot)$ be the MLLM output confidence. The feature similarity of x_i with another concept l can be represented as:

$$s_{kl} = q_w(x_i, l) \quad (4)$$

Then the feature similarity between two concepts labeled k and l can be approximated as:

$$\mathcal{S}_{kl} = \mathbb{E}(q_w(x_i, l)), (x_i, k) \in \mathcal{D}_{ex} \quad (5)$$

Subsequently, the transition possibilities of class k with all other concepts can be calculated through: $\mathbf{t}_k = (\mathcal{S}_{k1}, \mathcal{S}_{k2}, \dots, \mathcal{S}_{kK})^T / \sum_i^K \mathcal{S}_{ki}$. And the transition matrix \mathbf{T} , encoding all inter-conceptual similarities in \mathcal{D} , can be obtained via concatenation:

$$\mathbf{T} = (\mathbf{t}_1, \mathbf{t}_2, \dots, \mathbf{t}_K) \quad (6)$$

Figure 3 illustrates the transition matrix of CIFAR-10 as an example. Although it reflects the proportion of overlapped features among different concepts, this is not adequate for label re-assignment as a given instance does not necessarily express all the features belonging to its concept. Simply applying \mathbf{T} to assign perturbing labels will lead to biases followed by overfitting during unlearning. Therefore, it is essential to take the individual conditions of each instance into account.

Assigning perturbing labels Given the transition matrix \mathbf{T} , the overlapping of an instance x_i from class k with other concepts at the feature level can be computed via:

$$\mathbf{R}_i = \mathbf{T} \cdot (\tilde{\mathbf{I}}_k \cdot f_\theta(x_i)) \quad (7)$$

where $\tilde{\mathbf{I}}_k$ denotes an identity matrix with the elements of k -th row elements set to zero to avoid the influence of the original concept. And $f_\theta(x_i)$ denotes the softmax output logits of the pretrained model.

Consequently, the perturbing label for an instance $x_i \in \mathcal{D}_f$ is obtained by ranking elements of \mathbf{R}_i :

$$y_i^p = \phi(\mathbf{R}_i, \tau) \quad (8)$$

where $\phi(\cdot, \tau)$ denotes the process of selecting the top τ similar concept as the perturbing label. Here we set the parameter τ to control the distance between the target data and its re-assigned concept. As a perturbing concept that is too similar to the original one could fail to segregate the target data from the original embedding distribution, leading to insufficient unlearning. While the hindering of alignment with a too distant perturbing label will possibly cause model overfitting or representation collapse. In our experiments, we set $\tau = 0.3$ to ensure such a meaningful and alternative connection between target data and retained concepts. In Section E, we conduct detailed sensitivity studies for optimal hyperparameters.

To better understand the workflow of perturbing label generation, Algorithm 2 provides the detailed pseudo-code.

Algorithm 1 Transition matrix and perturbing labels.

Require: Instance x_i of class k from subset \mathcal{D}_{ex} selected from training set \mathcal{D} , concepts $\mathcal{Y} = \{0, 1, \dots, K-1\}$, MLLM q_w .
1: Let $q_w(x, y)$ represent the prompted MLLM output of image x and concept y .
2: **for** $k \in \mathcal{Y}$ **do**
3: **for** $l \in \mathcal{Y}$ **do**
4: $\tilde{\mathcal{S}}_{kl} = \frac{1}{n} \sum_i^n [q_w(x_i, l)], (x_i, k) \in \mathcal{D}_{ex}$ ▷ Eq. 5
5: **end for**
6: $\mathbf{t}_k = (\tilde{\mathcal{S}}_{k0}, \tilde{\mathcal{S}}_{k1}, \dots, \tilde{\mathcal{S}}_{kK-1})^T / \sum_i^{K-1} \tilde{\mathcal{S}}_{ki}$
7: **end for**
8: $\mathbf{T} = (\mathbf{t}_0, \mathbf{t}_1, \dots, \mathbf{t}_{K-1})$
Require: Instance (x_i, y_i) from forget set \mathcal{D}_f , transition matrix \mathbf{T} , class concepts $\mathcal{Y} = \{0, 1, \dots, K-1\}$, pretrained model p_θ , identity matrix \mathbf{I} of size $[K, K]$, constant τ .
9: Let $\phi(\cdot, \tau)$ denotes the process of selecting the index of the $\lfloor K\tau \rfloor$ -th largest element.
10: **for** $(x_i, y_i) \in \mathcal{D}_f$ **do**
11: $\tilde{\mathbf{I}}_{y_i} \leftarrow \mathbf{I}[j, y_i] = 0, j \in [0, K-1]$
12: $\mathbf{R}_i = \mathbf{T} \cdot [\tilde{\mathbf{I}}_{y_i} \cdot p_\theta(x_i)]$ ▷ Eq. 7
13: $y_i^p = \phi(\mathbf{R}_i, \tau)$
14: **end for**

The necessity of MLLM guidance for perturbing labels Here, we demonstrate why not use model predictions for label assignment instead of MLLM guidance. Due to the overconfidence, the predicted probabilities of the pretrained model on a class of target data will be concentrated on a very few labels, neglecting the semantic content of individual instances. This poses a risk of leading the pretrained model to overfit to a simple output bias. Conversely, our mechanism, considering individual conditions of target data, guarantees balanced perturbing labels. This facilitates the model in adjusting its decision boundaries according to different instances.

4.2 Target feature disentanglement and finetuning

In Section 1, we demonstrate that the key challenge of unlearning lies in feature entanglement: target data often share features with retained classes, which contributes to over-forgetting. To address this problem, we propose the

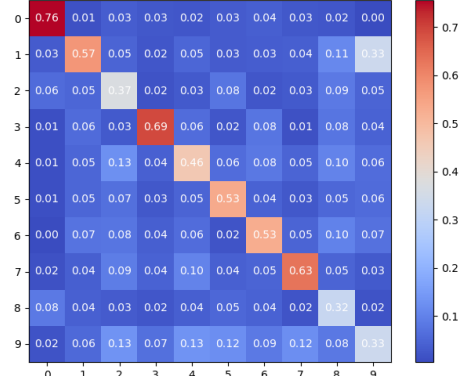


Figure 3: The visualized transition matrix.

distance between the target data and its re-assigned concept. As a perturbing concept that is too similar to the original one could fail to segregate the target data from the original embedding distribution, leading to insufficient unlearning. While the hindering of alignment with a too distant perturbing label will possibly cause model overfitting or representation collapse. In our experiments, we set $\tau = 0.3$ to ensure such a meaningful and alternative connection between target data and retained concepts. In Section E, we conduct detailed sensitivity studies for optimal hyperparameters.

To better understand the workflow of perturbing label generation, Algorithm 2 provides the detailed pseudo-code.

Require: Instance x_i of class k from subset \mathcal{D}_{ex} selected from training set \mathcal{D} , concepts $\mathcal{Y} = \{0, 1, \dots, K-1\}$, MLLM q_w .
1: Let $q_w(x, y)$ represent the prompted MLLM output of image x and concept y .
2: **for** $k \in \mathcal{Y}$ **do**
3: **for** $l \in \mathcal{Y}$ **do**
4: $\tilde{\mathcal{S}}_{kl} = \frac{1}{n} \sum_i^n [q_w(x_i, l)], (x_i, k) \in \mathcal{D}_{ex}$ ▷ Eq. 5
5: **end for**
6: $\mathbf{t}_k = (\tilde{\mathcal{S}}_{k0}, \tilde{\mathcal{S}}_{k1}, \dots, \tilde{\mathcal{S}}_{kK-1})^T / \sum_i^{K-1} \tilde{\mathcal{S}}_{ki}$
7: **end for**
8: $\mathbf{T} = (\mathbf{t}_0, \mathbf{t}_1, \dots, \mathbf{t}_{K-1})$
Require: Instance (x_i, y_i) from forget set \mathcal{D}_f , transition matrix \mathbf{T} , class concepts $\mathcal{Y} = \{0, 1, \dots, K-1\}$, pretrained model p_θ , identity matrix \mathbf{I} of size $[K, K]$, constant τ .
9: Let $\phi(\cdot, \tau)$ denotes the process of selecting the index of the $\lfloor K\tau \rfloor$ -th largest element.
10: **for** $(x_i, y_i) \in \mathcal{D}_f$ **do**
11: $\tilde{\mathbf{I}}_{y_i} \leftarrow \mathbf{I}[j, y_i] = 0, j \in [0, K-1]$
12: $\mathbf{R}_i = \mathbf{T} \cdot [\tilde{\mathbf{I}}_{y_i} \cdot p_\theta(x_i)]$ ▷ Eq. 7
13: $y_i^p = \phi(\mathbf{R}_i, \tau)$
14: **end for**

Fragment-Align strategy, which achieves semantic disentanglement through a pair of complementary feature noises. During fine-tuning, the **positive feature noise** \mathcal{N}^{pos} embeds features aligned with the perturbing label, encouraging the target instance to re-anchor toward the new concept and mitigating distributional gaps. Conversely, the **negative feature noise** \mathcal{N}^{neg} suppresses features tied to the original class, facilitating the destruction of target feature patterns in the model's latent space. Together, these two noises disentangle the target data from its original concept and realign it with the perturbed concept, facilitating the formation of new decision boundaries and enabling effective forgetting while preserving generalization on retained data.

Feature noise generation Specifically, given an instance from target data, its ground-truth label \mathcal{C}_{tar} and re-assigned perturbing label \mathcal{C}_{per} correspond respectively to feature patterns \mathcal{P}_{tar} and \mathcal{P}_{per} . We aim to eliminate the influence of the unique feature $\mathcal{P}_{tar}^{uni} = \mathcal{P}_{tar} \setminus \mathcal{P}_{tar|per}^{ass}$ while preserving shared features $\mathcal{P}_{tar|per}^{ass} = \mathcal{P}_{tar} \cap \mathcal{P}_{per}$ from unexpected disruption.

Here, we demonstrate the derivation of feature noises. Let f_θ be the pre-trained model, (x_i, y_i) be an instance from forget data, y_i^p be the perturbing label. The \mathcal{N} is a randomly initialized matrix. The positive feature noise can be obtained through minimizing the loss function towards the perturbing label y_i^p while freezing the pretrained model:

$$\mathcal{N}_i^{pos} = \arg \min_{\mathcal{N}} \mathbb{E}(\mathcal{L}(f_\theta(\mathcal{N}), y_i^p) + \lambda \|w_{noise}\|) \quad (9)$$

Similarly, the negative feature noise can be obtained by changing the training direction towards the original label y_i with a conversed loss function:

$$\mathcal{N}_i^{neg} = \arg \min_{\mathcal{N}} \mathbb{E}(-\mathcal{L}(f_\theta(\mathcal{N}), y_i) + \lambda \|w_{noise}\|) \quad (10)$$

Through this process, \mathcal{N}_i^{pos} gradually aligns with the direction of gradient descent, thereby capturing and perturbing features associated with the noisy label y_i^p . On the other hand, \mathcal{N}_i^{neg} is driven toward the direction of gradient ascent in the model's optimization landscape to extract counteracting feature information opposite to the target data from the pretrained model. When jointly used with the target forgetting data during model re-optimization, the perturbing-label-related features embedded in \mathcal{N}_i^{pos} strengthen the semantic association between the target data features and the perturbed label concept, helping construct alternative connections other than those originally learned during model pre-training. Meanwhile, as the model's behavior to \mathcal{N}_i^{neg} is re-optimized in a gradient descent manner, its capability to recognize features associated with the target concept is therefore disrupted.

Model re-optimization Intuitively, both the unique and associated feature patterns from concept y_i are restrained by \mathcal{N}_i^{neg} . Simultaneously, the associated feature patterns shared with y_i^p are restored by \mathcal{N}_i^{pos} . Therefore, by adjusting the relative weights of \mathcal{N}_i^{pos} and \mathcal{N}_i^{neg} , the injected feature noises can be precisely controlled to suppress the unique features of the target data, preserve the associated features shared between the target data and the perturbed concept, and introduce new perturbing-label-related features that facilitate aligning the model's input with the perturbed labels.

Specifically, incorporated with perturbing labels, the perturbed forget dataset is formulated as $\mathcal{D}_f^p = \{(x_i + \mathcal{N}_i, y_i^p) | x_i \in \mathcal{D}_f\}$, where \mathcal{N}_i represents the weighted combination of positive and negative noises:

$$\mathcal{N}_i = \alpha \mathcal{N}_i^{pos} + (1 - \alpha) \mathcal{N}_i^{neg} \quad (11)$$

where the constant α serves as a control parameter determining the weights of feature noises. Empirically, we set $\alpha = 0.7$ according to the results of sensitivity study in Section E. Note that the feature noises can be pre-generated prior to the unlearning stages and reused across subsequent iterations to reduce computational and time costs.

At the finetuning stage, we aim to change the model optimization direction shown in Equation 1 through a perturbed dataset \mathcal{D}_f^p , where representations of target data are pulled away from the original distribution and towards the retained data points. Specifically, the unlearning objective is achieved through updating model parameters where θ' denotes the updated parameters:

$$\theta' = \arg \min_{\theta'} \left\{ \begin{array}{l} \sum_{(x_i, y_i^p) \in \mathcal{D}_f^p} \mathcal{L}(f_\theta(x_i + \mathcal{N}_i), y_i^p) \\ \sum_{(x_i, y_i) \in \mathcal{D}_r} \mathcal{L}(f_\theta(x_i), y_i) \end{array} \right\} \quad (12)$$

This process reshapes the decision boundaries with alternative embedding distributions. At the same time, the combination of positive and negative feature noises prevents the realignment from disrupting other data points via the disentanglement of target data features, where the positive feature noise additionally smooths the re-optimization. In Section F, we further explore the effects of these two components and the distinct roles of the two kinds of feature noises respectively through ablation studies.

Table 1: Class-wise unlearning on CIFAR-100.

model	class	metric	baseline	retrain	FT	UNSIR	AMNC	SSD	MaGA
RN18	RKT	A_r	76.30	76.19	65.43	73.83	73.59	75.86	75.75
		A_f	82.81	0.00	0.00	41.15	0.00	0.00	0.00
		MIA	96.61	8.06	10.04	3.08	28.62	0.66	0.00
	MR	A_r	76.38	76.23	63.90	74.26	73.22	76.20	76.25
		A_f	82.03	0.00	0.00	8.07	0.00	0.00	0.00
		MIA	95.65	6.01	12.22	1.68	46.06	0.25	0.00
ViT	RKT	A_r	92.27	92.04	84.26	90.83	90.53	91.39	92.34
		A_f	93.14	0.00	0.00	24.57	0.00	0.00	0.00
		MIA	84.88	6.29	16.00	11.43	1.06	6.62	0.00
	MR	A_r	92.20	92.18	84.15	89.95	89.95	91.78	92.33
		A_f	98.44	0.00	0.00	56.25	0.00	0.00	0.00
		MIA	90.24	0.86	5.05	2.61	0.88	1.45	0.00

Table 2: Class-wise unlearning on CIFAR-20.

model	class	metric	baseline	retrain	FT	UNSIR	AMNC	SSD	MaGA
RN18	veh2	A_r	82.84	82.41	73.74	81.41	82.21	83.38	82.93
		A_f	84.99	0.00	0.00	58.82	0.00	22.37	0.00
		MIA	87.72	14.24	40.84	45.68	7.84	5.72	0.08
	veg	A_r	82.59	82.24	72.56	81.23	81.66	82.64	82.53
		A_f	88.94	0.00	0.00	70.24	0.00	45.34	0.00
		MIA	93.28	9.24	29.16	43.27	3.04	2.08	0.00
ViT	veh2	A_r	96.08	95.35	85.13	93.83	94.20	90.26	95.82
		A_f	94.35	0.00	0.00	67.29	0.00	0.00	0.00
		MIA	80.96	20.36	22.00	49.96	1.26	9.88	0.00
	veg	A_r	95.88	94.95	88.52	93.75	93.31	95.61	95.64
		A_f	97.67	0.00	0.59	86.57	0.00	0.00	0.00
		MIA	91.48	4.16	14.44	63.6	1.05	1.44	0.00

5 Experiments

In this section, we demonstrate experimental results on different unlearning tasks and datasets and compare the performance of MaGA with existing methods using a set of metrics. We randomly sample 10,000 instances from the retain dataset \mathcal{D}_r along with the perturbed forget set \mathcal{D}_f^p for fine-tuning using Eq. 12. We perform 3 epochs of unlearning for ResNet18, and 5 epochs for Vision Transformer (ViT). While increasing the number of unlearning epochs will further enhance performance, it comes at the expense of computational efficiency. Note that the metrics in tables are represented as percentages, and the boldings indicate superiority. For detailed hyper-parameter settings, we conduct sensitivity in Appendix E. To better understand the effects of perturbing labels and feature noises, we conduct ablation studies in the Appendix F by comparing MaGA with a randomly-selecting perturbing label strategy and a none feature noise framework. We also visualize the predictions of unlearned models compared with the "gold model" and baseline model to demonstrate the effects of unlearning in Appendix D. More results of class-wise and sub-class unlearning experiments on other target data are also present in Appendix G.

5.1 Experimental setup

Datasets: Following [Foster et al., 2024], we evaluate our proposed method for image classification models using CIFAR-10, CIFAR-100 [Krizhevsky et al., 2009], CIFAR-20 [Xie et al., 2020].

Models: We leverage MMICL [Zhao et al., 2023b] as our MLLM zero-shot machine expert. We conduct unlearning experiments on two types of backbones: ResNet18 [He et al., 2016] and Vision Transformer (ViT) [Dosovitskiy, 2020]. Models are trained using Adam optimizer [Diederik, 2014] and a multi-step scheduler with the initial learning rate set to 0.1. In convenience of comparisons, we control the training of the baseline model to align with that of the previous studies. The pretraining and unlearning processes are carried out on NVIDIA RTX4090 and Intel Xeon platform. The memory usage is controlled within 30 GiB for MLLM inference and less for unlearning.

Table 3: Sub-class unlearning on CIFAR-20.

model	sublass	metric	baseline	retrain	FT	UNSIR	AMNC	SSD	MaGA
RN18	RKT	A_r	82.93	83.55	73.57	81.50	81.89	82.36	82.44
		A_f	81.51	1.39	15.36	60.85	0.00	5.90	4.51
		MIA	84.43	22.40	12.29	43.6	9.41	5.85	4.80
	sea	A_r	82.79	82.95	85.85	81.14	82.06	82.41	82.80
		A_f	97.66	77.34	76.14	95.49	35.76	86.02	84.38
		MIA	87.10	56.67	66.05	86.60	4.00	54.65	66.68
ViT	RKT	A_r	96.01	96.10	88.61	93.59	92.39	96.18	96.05
		A_f	94.70	2.83	5.12	66.75	0.78	22.83	1.10
		MIA	85.80	7.44	19.41	15.47	0.86	3.45	0.00
	sea	A_r	95.97	95.55	88.47	94.28	93.82	95.96	96.05
		A_f	98.44	74.22	81.68	89.15	17.97	97.66	12.76
		MIA	89.26	41.43	43.27	69.20	0.22	86.49	0.20

Table 4: Random unlearning on CIFAR-10.

model	metric	baseline	retrain	FT	teacher	AMNC	SSD	MaGA
RN18	A_r	95.31	92.42	87.86	90.68	90.63	91.38	93.04
	A_f	94.03	94.40	88.77	93.13	55.35	95.88	85.59
	MIA	76.53	74.42	71.70	47.08	17.89	76.50	34.04
ViT	A_r	98.66	98.75	97.64	98.17	98.15	98.63	98.81
	A_f	99.71	99.41	98.24	93.52	74.88	99.39	96.27
	MIA	88.66	91.67	86.83	26.80	6.40	88.22	29.18

Unlearning tasks: Following previous studies [Foster et al., 2024, Chundawat et al., 2023, Tarun et al., 2023], we evaluate the effectiveness of MaGA across three distinct unlearning tasks, including: 1) Class-wise unlearning conducted on CIFAR-100 and CIFAR-20, which unlearns an entire superclass from the dataset. 2) Sub-class unlearning conducted on CIFAR-20, where a sub-class within a superclass is forgotten. 3) Random unlearning conducted on CIFAR-10 where a subset randomly selected from the original dataset is forgotten.

Baselines: Following previous researches [Foster et al., 2024, Graves et al., 2021], we compare our method with baselines including: "baseline": the original pre-trained model, "retrain": the gold model trained from scratch, "FT" which finetunes the pre-trained model for 5 epochs with only retain data, "UNSIR" [Tarun et al., 2023], "teacher" which denotes Bad Teacher [Chundawat et al., 2023], "AMNC" which denotes Amnesiac [Graves et al., 2021], and "SSD" [Foster et al., 2024].

Evaluation metrics: Following [Chundawat et al., 2023], we use: 1) Accuracy on forget and retain set, denoted as A_f and A_r respectively; 2) Membership Inference Attack (MIA) score [Shokri et al., 2017] as evaluating metrics. Considering the Streisand effect [Chundawat et al., 2023], we demonstrate that the unlearned model that aligns close to the gold model on accuracy is "well-unlearned". Meanwhile, lower MIA probabilities indicate better security in adversary attacks.

5.2 Main implementation results

Class-wise unlearning: Experiments are conducted on CIFAR-100 and CIFAR-20 using ResNet18 and Vision Transformer as classification backbones. For CIFAR-100, we designate two classes: *rocket* (denoted as "RKT") and *mushroom* (denoted as "MR"). The results are shown in Table 1. Metrics demonstrate that our method successfully aligns its performance with the "gold model" denoted as "retrain". Especially when class-wisely unlearning *rocket* using ViT, MaGA narrows the gap with retrained model in retain accuracy by 0.35% compared to *SSD*. For CIFAR-20, we forget two superclasses: *Vehicle2* and *veg*. MaGA evidently lowers the retain accuracy compared with previous methods such as *SSD*, particularly decreasing over 40% on *vegetable* using ResNet18. Meanwhile, MaGA still maintains a competitive retain accuracy of 82.53%, which is closer to 82.24% of the "gold model". Thus, it is demonstrated that MaGA achieves a balance between complete unlearning and preservation of overall generalization. Crucially, MaGA significantly lowers the MIA risk compared to existing methods on most tasks, with 9.8% and 49% lower than *SSD* and *UNSIR* respectively on *veh2* from CIFAR-20 using ViT. This highlights the effectiveness of removing target information without being recognized by adversaries.

Sub-class unlearning: We perform unlearning on two sub-classes: *rocket* and *sea*, belonging to the super-classes "Vehicle2" and "natural scenes", respectively. The results are summarized in Table 3. The challenge of sub-class unlearning exists that the target sub-class shares feature patterns with fellows within the same super-class. Thus, when the features of the target sub-class are unlearned, the generalization capabilities of the entire super-class are compromised. This is evident in methods such as *UNSIR* and *Amnesiac*, which exhibit significant reductions in retain accuracy. In contrast, benefiting from the disentanglement of Fragment-Align strategy, the performance of MaGA on retained data can be well preserved and closely aligned with the "gold model". Taking sub-class *rocket* with ViT backbone as an example, MaGA increases the retain accuracy by 2.51% and 3.71% compared to *UNSIR* and *Amnesiac* respectively. The superiority of MIA security of MaGA unlearning is also recurrently demonstrated among these cases, especially 86% and 69% lower than that of *SSD* and *UNSIR* on *sea* with ViT.

Random unlearning: We utilize the CIFAR-10 dataset for random unlearning, where a set of instances (100 in our experiments) is randomly selected as the target dataset to be forgotten. As shown in Table 4, random unlearning is inherently more difficult as the retrained gold model also persists a relatively high forget accuracy. In random unlearning, the forget set and retain set may contain samples from the same semantic class. Thus the unlearned model preserves generalization capability toward the class, making it possible to correctly classify forgotten samples despite their removal. More importantly, this indicates that, in such settings, the unlearning performance cannot be fully measured by accuracy alone. In this case, MaGA competitively reduces MIA scores compared to most baselines and the gold model, with 40% and 79% lower than *SSD* using ResNet18 and ViT respectively, which suggests that the model no longer remembers specific target instances, despite still leveraging general class-level knowledge. Simultaneously, it is still illustrated that MaGA behaves closely to the "gold model", with the overall generalization preserved after unlearning.

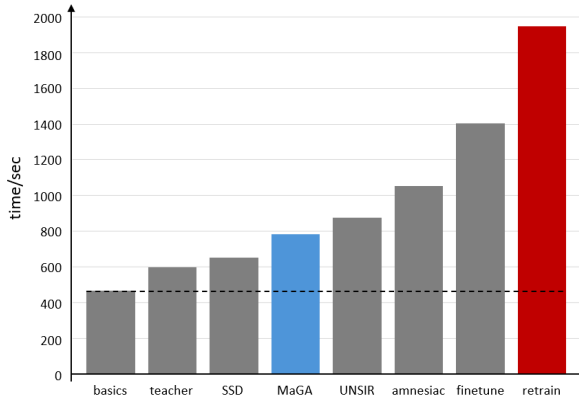


Figure 4: Time consumed for CIFAR-100 class-wise unlearning.

Computation time: We evaluate the time required to complete the unlearning process for each method, where the "basics" accounts for the time spent on dataset preparation, model loading, and metric computation. Using CIFAR-100 class-wise unlearning with the Vision Transformer (ViT) backbone as an example, MaGA reduces computational time by over 59% compared to full retraining, as illustrated in Figure 4.

6 Conclusion

Contributions: In this work, we introduce MeGU, a novel machine unlearning framework that effectively eliminate target data influence while maintaining overall model generalization through pioneering feature disentanglement and data realignment under the guidance of MLLMs. Extensive experiments across diverse datasets and forgetting tasks validate that MeGU consistently outperforms existing unlearning methods under most conditions, ensuring secured and effective unlearning. In future work, this framework can be extended to accommodate more complex unlearning scenarios and a broader range of pre-trained models.

Limitations: Due to the computation cost of utilizing MLLMs, MeGU is not the most time-efficient unlearning approaches. Nevertheless, this limitation can be mitigated through several strategies: 1) employing zero-shot inference from MLLMs solely as a form of knowledge guidance; 2) precomputing conceptual similarities and the transition matrix for a given dataset prior to the occurrence of any unlearning requests, and subsequently reusing the obtained transition matrix across all future unlearning tasks. Furthermore, the number of exemplars used in estimating the transition matrix can be flexibly adjusted to further reduce computational costs.

References

Michael I Jordan and Tom M Mitchell. Machine learning: Trends, perspectives, and prospects. *Science*, 349(6245): 255–260, 2015.

Dengsheng Lu and Qihao Weng. A survey of image classification methods and techniques for improving classification performance. *International journal of Remote sensing*, 28(5):823–870, 2007.

Prakash M Nadkarni, Lucila Ohno-Machado, and Wendy W Chapman. Natural language processing: an introduction. *Journal of the American Medical Informatics Association*, 18(5):544–551, 2011.

Marija Jegorova, Chaitanya Kaul, Charlie Mayor, Alison Q O’Neil, Alexander Weir, Roderick Murray-Smith, and Sotirios A Tsaftaris. Survey: Leakage and privacy at inference time. *IEEE Transactions on Pattern Analysis and Machine Intelligence*, 45(7):9090–9108, 2022.

Shaopeng Fu, Fengxiang He, and Dacheng Tao. Knowledge removal in sampling-based bayesian inference. *arXiv preprint arXiv:2203.12964*, 2022.

Cynthia Dwork, Aaron Roth, et al. The algorithmic foundations of differential privacy. *Foundations and Trends® in Theoretical Computer Science*, 9(3–4):211–407, 2014.

Jacob Steinhardt, Pang Wei W Koh, and Percy S Liang. Certified defenses for data poisoning attacks. *Advances in neural information processing systems*, 30, 2017.

Paul Voigt and Axel Von dem Bussche. The eu general data protection regulation (gdpr). *A Practical Guide, 1st Ed.*, Cham: Springer International Publishing, 10(3152676):10–5555, 2017.

Rob Bonta. California consumer privacy act (ccpa). *Retrieved from State of California Department of Justice: https://oag.ca.gov/privacy/ccpa*, 2022.

Jeffrey Rosen. The right to be forgotten. *Stan. L. Rev. Online*, 64:88, 2011.

Emmie Hine, Claudio Novelli, Mariarosaria Taddeo, and Luciano Floridi. Supporting trustworthy ai through machine unlearning. *Science and Engineering Ethics*, 30(5):43, 2024.

James Jin Kang, Dang Bui, Thanh Pham, and Huo-Chong Ling. Unlearning imperative: Securing trustworthy and responsible llms through engineered forgetting. *arXiv preprint arXiv:2511.09855*, 2025.

Zhuo Huang. Trustworthy machine learning under distribution shifts. *arXiv preprint arXiv:2512.23524*, 2025.

Haoyu Wang, Zhuo Huang, Zhiwei Lin, and Tongliang Liu. Noisegpt: Label noise detection and rectification through probability curvature. In *The Thirty-eighth Annual Conference on Neural Information Processing Systems*, 2024a.

Mingyu Li, Tao Zhou, Zhuo Huang, Jian Yang, Jie Yang, and Chen Gong. Dynamic weighted adversarial learning for semi-supervised classification under intersectional class mismatch. *ACM Transactions on Multimedia Computing, Communications and Applications*, 20(4):1–24, 2024.

Suqin Yuan, Lei Feng, and Tongliang Liu. Early stopping against label noise without validation data. In *The Twelfth International Conference on Learning Representations*, 2024.

Suqin Yuan, Lei Feng, Bo Han, and Tongliang Liu. Enhancing sample selection against label noise by cutting mislabeled easy examples. In *The Thirty-ninth Annual Conference on Neural Information Processing Systems*, 2025.

Lucas Bourtoule, Varun Chandrasekaran, Christopher A Choquette-Choo, Hengrui Jia, Adelin Travers, Baiwu Zhang, David Lie, and Nicolas Papernot. Machine unlearning. In *2021 IEEE Symposium on Security and Privacy (SP)*, pages 141–159. IEEE, 2021.

Haonan Yan, Xiaoguang Li, Ziyao Guo, Hui Li, Fenghua Li, and Xiaodong Lin. Arcane: An efficient architecture for exact machine unlearning. In *IJCAI*, volume 6, page 19, 2022.

Ayush Sekhari, Jayadev Acharya, Gautam Kamath, and Ananda Theertha Suresh. Remember what you want to forget: Algorithms for machine unlearning. *Advances in Neural Information Processing Systems*, 34:18075–18086, 2021.

Ming Zhao, Meng Li, Sheng-Lung Peng, and Jie Li. A novel deep learning model compression algorithm. *Electronics*, 11(7):1066, 2022.

Aditya Golatkar, Alessandro Achille, and Stefano Soatto. Eternal sunshine of the spotless net: Selective forgetting in deep networks. In *Proceedings of the IEEE/CVF Conference on Computer Vision and Pattern Recognition*, pages 9304–9312, 2020a.

Takashi Shibata, Go Irie, Daiki Ikami, and Yu Mitsuzumi. Learning with selective forgetting. In *IJCAI*, volume 3, page 4, 2021.

Yinjun Wu, Edgar Dobriban, and Susan Davidson. Deltagrad: Rapid retraining of machine learning models. In *International Conference on Machine Learning*, pages 10355–10366. PMLR, 2020.

Zhuo Huang, Qizhou Wang, Ziming Hong, Shanshan Ye, Bo Han, and Tongliang Liu. Is gradient ascent really necessary? memorize to forget for machine unlearning. *arXiv preprint arXiv:2602.06441*, 2026.

Laura Graves, Vineel Nagisetty, and Vijay Ganesh. Amnesiac machine learning. In *Proceedings of the AAAI Conference on Artificial Intelligence*, volume 35, pages 11516–11524, 2021.

Ayush K Tarun, Vikram S Chundawat, Murari Mandal, and Mohan Kankanhalli. Fast yet effective machine unlearning. *IEEE Transactions on Neural Networks and Learning Systems*, 2023.

Haotian Ye, Chuanlong Xie, Tianle Cai, Ruichen Li, Zhenguo Li, and Liwei Wang. Towards a theoretical framework of out-of-distribution generalization. *Advances in Neural Information Processing Systems*, 34:23519–23531, 2021.

Zhuo Huang, Xiaobo Xia, Li Shen, Bo Han, Mingming Gong, Chen Gong, and Tongliang Liu. Harnessing out-of-distribution examples via augmenting content and style. In *The Eleventh International Conference on Learning Representations*, 2023. URL <https://openreview.net/forum?id=boNyg20-JDm>.

Zhuo Huang, Gang Niu, Bo Han, Masashi Sugiyama, and Tongliang Liu. Towards out-of-modal generalization without instance-level modal correspondence. In *The Thirteenth International Conference on Learning Representations*, 2025.

Joan Serra, Didac Suris, Marius Miron, and Alexandros Karatzoglou. Overcoming catastrophic forgetting with hard attention to the task. In *International conference on machine learning*, pages 4548–4557. PMLR, 2018.

Wenhan Chang, Tianqing Zhu, Heng Xu, Wenjian Liu, and Wanlei Zhou. Class machine unlearning for complex data via concepts inference and data poisoning. *arXiv preprint arXiv:2405.15662*, 2024.

Min Chen, Weizhuo Gao, Gaoyang Liu, Kai Peng, and Chen Wang. Boundary unlearning: Rapid forgetting of deep networks via shifting the decision boundary. In *Proceedings of the IEEE/CVF Conference on Computer Vision and Pattern Recognition*, pages 7766–7775, 2023.

Haotian Liu, Chunyuan Li, Qingyang Wu, and Yong Jae Lee. Visual instruction tuning. *Advances in neural information processing systems*, 36, 2024a.

Zhuo Huang, Chang Liu, Yinpeng Dong, Hang Su, Shibao Zheng, and Tongliang Liu. Machine vision therapy: Multimodal large language models can enhance visual robustness via denoising in-context learning. In *Forty-first International Conference on Machine Learning*, 2024. URL <https://openreview.net/forum?id=Lw0fVWgEzS>.

Ziming Hong, Zhenyi Wang, Li Shen, Yu Yao, Zhuo Huang, Shiming Chen, Chuanwu Yang, Mingming Gong, and Tongliang Liu. Improving non-transferable representation learning by harnessing content and style. In *The Twelfth International Conference on Learning Representations*, 2024.

Ziming Hong, Shiming Chen, Guo-Sen Xie, Wenhan Yang, Jian Zhao, Yuanjie Shao, Qinmu Peng, and Xinge You. Semantic compression embedding for generative zero-shot learning. In *IJCAI*, volume 7, pages 956–963, 2022.

Shiming Chen, Ziming Hong, Xinge You, and Ling Shao. Semantics-conditioned generative zero-shot learning via feature refinement. *International Journal of Computer Vision*, pages 1–18, 2025.

Zhiwen Zhou, Ximeng Liu, Jiayin Li, Junxi Ruan, and Mingyuan Fan. Dynamically selected mixup machine unlearning. In *2022 IEEE International Conference on Trust, Security and Privacy in Computing and Communications (TrustCom)*, pages 514–524. IEEE, 2022.

Jonathan Brophy and Daniel Lowd. Machine unlearning for random forests. In *International Conference on Machine Learning*, pages 1092–1104. PMLR, 2021.

Jiancheng Liu, Parikshit Ram, Yuguang Yao, Gaowen Liu, Yang Liu, PRANAY SHARMA, Sijia Liu, et al. Model sparsity can simplify machine unlearning. *Advances in Neural Information Processing Systems*, 36, 2024b.

Junxiao Wang, Song Guo, Xin Xie, and Heng Qi. Federated unlearning via class-discriminative pruning. In *Proceedings of the ACM Web Conference 2022*, pages 622–632, 2022.

Hidegori Tanaka, Daniel Kunin, Daniel L Yamins, and Surya Ganguli. Pruning neural networks without any data by iteratively conserving synaptic flow. *Advances in neural information processing systems*, 33:6377–6389, 2020.

Vitaly Feldman. Does learning require memorization? a short tale about a long tail. In *Proceedings of the 52nd Annual ACM SIGACT Symposium on Theory of Computing*, pages 954–959, 2020.

Cory Stephenson, Suchismita Padhy, Abhinav Ganesh, Yue Hui, Hanlin Tang, and SueYeon Chung. On the geometry of generalization and memorization in deep neural networks. *arXiv preprint arXiv:2105.14602*, 2021.

Seul-Ki Yeom, Philipp Seegerer, Sebastian Lapuschkin, Alexander Binder, Simon Wiedemann, Klaus-Robert Müller, and Wojciech Samek. Pruning by explaining: A novel criterion for deep neural network pruning. *Pattern Recognition*, 115:107899, 2021.

Xiaolong Ma, Geng Yuan, Xuan Shen, Tianlong Chen, Xuxi Chen, Xiaohan Chen, Ning Liu, Minghai Qin, Sijia Liu, Zhangyang Wang, et al. Sanity checks for lottery tickets: Does your winning ticket really win the jackpot? *Advances in Neural Information Processing Systems*, 34:12749–12760, 2021.

Jonathan Frankle and Michael Carbin. The lottery ticket hypothesis: Finding sparse, trainable neural networks. *arXiv preprint arXiv:1803.03635*, 2018.

Ga Wu, Masoud Hashemi, and Christopher Srinivasa. Puma: Performance unchanged model augmentation for training data removal. In *Proceedings of the AAAI conference on artificial intelligence*, volume 36, pages 8675–8682, 2022.

Vinith Suriyakumar and Ashia C Wilson. Algorithms that approximate data removal: New results and limitations. *Advances in Neural Information Processing Systems*, 35:18892–18903, 2022.

Jack Foster, Stefan Schoepf, and Alexandra Brintrup. Fast machine unlearning without retraining through selective synaptic dampening. In *Proceedings of the AAAI Conference on Artificial Intelligence*, volume 38, pages 12043–12051, 2024.

Puning Yang, Qizhou Wang, Zhuo Huang, Tongliang Liu, Chengqi Zhang, and Bo Han. Exploring criteria of loss reweighting to enhance ILM unlearning. In *Forty-second International Conference on Machine Learning*, 2025. URL <https://openreview.net/forum?id=mG0ugCZ1Aq>.

Seth Neel, Aaron Roth, and Saeed Sharifi-Malvajerdi. Descent-to-delete: Gradient-based methods for machine unlearning. In *Algorithmic Learning Theory*, pages 931–962. PMLR, 2021.

Xiaoyu Cao, Jinyuan Jia, Zaixi Zhang, and Neil Zhenqiang Gong. Fedrecover: Recovering from poisoning attacks in federated learning using historical information. In *2023 IEEE Symposium on Security and Privacy (SP)*, pages 1366–1383. IEEE, 2023.

Thanveer Shaik, Xiaohui Tao, Haoran Xie, Lin Li, Xiaofeng Zhu, and Qing Li. Exploring the landscape of machine unlearning: A comprehensive survey and taxonomy. *IEEE Transactions on Neural Networks and Learning Systems*, 2024.

Chongyu Fan, Jiancheng Liu, Yihua Zhang, Eric Wong, Dennis Wei, and Sijia Liu. Salun: Empowering machine unlearning via gradient-based weight saliency in both image classification and generation. *arXiv preprint arXiv:2310.12508*, 2023.

Yue Wang, Qizhou Wang, Zizhuo Zhang, Ang Li, Gang Niu, Bo Han, and Masashi Sugiyama. What is preference optimization doing, how and why? *Arxiv Preprint*, 2025a.

Yue Wang, Qizhou Wang, Feng Liu, Wei Huang, Yali Du, Xiaojiang Du, and Bo Han. Gru: Mitigating the trade-off between unlearning and retention for large language models. In *International Conference on Machine Learning*, 2025b.

Aditya Golatkar, Alessandro Achille, Avinash Ravichandran, Marzia Polito, and Stefano Soatto. Mixed-privacy forgetting in deep networks. In *Proceedings of the IEEE/CVF conference on computer vision and pattern recognition*, pages 792–801, 2021.

Aditya Golatkar, Alessandro Achille, and Stefano Soatto. Forgetting outside the box: Scrubbing deep networks of information accessible from input-output observations. In *Computer Vision–ECCV 2020: 16th European Conference, Glasgow, UK, August 23–28, 2020, Proceedings, Part XXIX 16*, pages 383–398. Springer, 2020b.

Ronak Mehta, Sourav Pal, Vikas Singh, and Sathya N Ravi. Deep unlearning via randomized conditionally independent Hessians. In *Proceedings of the IEEE/CVF Conference on Computer Vision and Pattern Recognition*, pages 10422–10431, 2022.

Ryutaro Tanno, Melanie F Pradier, Aditya Nori, and Yingzhen Li. Repairing neural networks by leaving the right past behind. *Advances in Neural Information Processing Systems*, 35:13132–13145, 2022.

Yang Liu, Mingyuan Fan, Cen Chen, Ximeng Liu, Zuo Ma, Li Wang, and Jianfeng Ma. Backdoor defense with machine unlearning. In *IEEE INFOCOM 2022-IEEE conference on computer communications*, pages 280–289. IEEE, 2022.

Qizhou Wang, Yong Lin, Yongqiang Chen, Ludwig Schmidt, Bo Han, and Tong Zhang. A sober look at the robustness of clips to spurious features. *Advances in Neural Information Processing Systems*, 37:122484–122523, 2024b.

Vikram S Chundawat, Ayush K Tarun, Murari Mandal, and Mohan Kankanhalli. Can bad teaching induce forgetting? unlearning in deep networks using an incompetent teacher. In *Proceedings of the AAAI Conference on Artificial Intelligence*, volume 37, pages 7210–7217, 2023.

Xulong Zhang, Jianzong Wang, Ning Cheng, Yifu Sun, Chuanyao Zhang, and Jing Xiao. Machine unlearning methodology based on stochastic teacher network. In *International Conference on Advanced Data Mining and Applications*, pages 250–261. Springer, 2023.

Shen Lin, Xiaoyu Zhang, Chenyang Chen, Xiaofeng Chen, and Willy Susilo. Erm-ktp: Knowledge-level machine unlearning via knowledge transfer. In *Proceedings of the IEEE/CVF Conference on Computer Vision and Pattern Recognition*, pages 20147–20155, 2023.

Zhuo Huang, Jian Yang, and Chen Gong. They are not completely useless: Towards recycling transferable unlabeled data for class-mismatched semi-supervised learning. *IEEE Transactions on Multimedia*, 2022.

A Vaswani. Attention is all you need. *Advances in Neural Information Processing Systems*, 2017.

Tom B Brown. Language models are few-shot learners. *arXiv preprint arXiv:2005.14165*, 2020.

Luciano Floridi and Massimo Chiriatti. Gpt-3: Its nature, scope, limits, and consequences. *Minds and Machines*, 30: 681–694, 2020.

Hugo Touvron, Thibaut Lavril, Gautier Izacard, Xavier Martinet, Marie-Anne Lachaux, Timothée Lacroix, Baptiste Rozière, Naman Goyal, Eric Hambro, Faisal Azhar, et al. Llama: Open and efficient foundation language models. *arXiv preprint arXiv:2302.13971*, 2023a.

Hugo Touvron, Louis Martin, Kevin Stone, Peter Albert, Amjad Almahairi, Yasmine Babaei, Nikolay Bashlykov, Soumya Batra, Prajjwal Bhargava, Shruti Bhosale, et al. Llama 2: Open foundation and fine-tuned chat models. *arXiv preprint arXiv:2307.09288*, 2023b.

Alexey Dosovitskiy. An image is worth 16x16 words: Transformers for image recognition at scale. *arXiv preprint arXiv:2010.11929*, 2020.

Junnan Li, Dongxu Li, Caiming Xiong, and Steven Hoi. Blip: Bootstrapping language-image pre-training for unified vision-language understanding and generation. In *International conference on machine learning*, pages 12888–12900. PMLR, 2022.

Junnan Li, Dongxu Li, Silvio Savarese, and Steven Hoi. Blip-2: Bootstrapping language-image pre-training with frozen image encoders and large language models. In *International conference on machine learning*, pages 19730–19742. PMLR, 2023.

Wenliang Dai, Junnan Li, D Li, AMH Tiong, J Zhao, W Wang, B Li, P Fung, and S Hoi. Instructblip: Towards general-purpose vision-language models with instruction tuning. *arXiv 2023*. *arXiv preprint arXiv:2305.06500*, 2, 2023.

Qinghao Ye, Haiyang Xu, Guohai Xu, Jiabo Ye, Ming Yan, Yiyang Zhou, Junyang Wang, Anwen Hu, Pengcheng Shi, Yaya Shi, et al. mplug-owl: Modularization empowers large language models with multimodality. *arXiv preprint arXiv:2304.14178*, 2023.

Shivam Garg, Dimitris Tsipras, Percy S Liang, and Gregory Valiant. What can transformers learn in-context? a case study of simple function classes. *Advances in neural information processing systems*, 35:30583–30598, 2022.

Sang Michael Xie, Aditi Raghunathan, Percy Liang, and Tengyu Ma. An explanation of in-context learning as implicit bayesian inference. *arXiv preprint arXiv:2111.02080*, 2021.

Haozhe Zhao, Zefan Cai, Shuzheng Si, Xiaojian Ma, Kaikai An, Liang Chen, Zixuan Liu, Sheng Wang, Wenjuan Han, and Baobao Chang. Mmicl: Empowering vision-language model with multi-modal in-context learning. *arXiv preprint arXiv:2309.07915*, 2023a.

Jean-Baptiste Alayrac, Jeff Donahue, Pauline Luc, Antoine Miech, Iain Barr, Yana Hasson, Karel Lenc, Arthur Mensch, Katherine Millican, Malcolm Reynolds, et al. Flamingo: a visual language model for few-shot learning. *Advances in neural information processing systems*, 35:23716–23736, 2022.

Laith Alzubaidi, Jinglan Zhang, Amjad J Humaidi, Ayad Al-Dujaili, Ye Duan, Omran Al-Shamma, José Santamaría, Mohammed A Fadhel, Muthana Al-Amidie, and Laith Farhan. Review of deep learning: concepts, cnn architectures, challenges, applications, future directions. *Journal of big Data*, 8(1):53, 2021.

Zeyuan Allen-Zhu and Yuanzhi Li. Backward feature correction: How deep learning performs deep (hierarchical) learning. In *The Thirty Sixth Annual Conference on Learning Theory*, pages 4598–4598. PMLR, 2023.

Alex Krizhevsky, Geoffrey Hinton, et al. Learning multiple layers of features from tiny images. 2009.

Qizhe Xie, Zihang Dai, Eduard Hovy, Thang Luong, and Quoc Le. Unsupervised data augmentation for consistency training. *Advances in neural information processing systems*, 33:6256–6268, 2020.

Haoyang Zhao, Zefan Cai, Shuzheng Si, Xiaojian Ma, Kaikai An, Liang Chen, Zixuan Liu, Sheng Wang, Wenjuan Han, and Baobao Chang. Mmicl: Empowering vision-language model with multi-modal in-context learning. *arXiv preprint arXiv:2309.07915*, 2023b.

Kaiming He, Xiangyu Zhang, Shaoqing Ren, and Jian Sun. Deep residual learning for image recognition. In *Proceedings of the IEEE conference on computer vision and pattern recognition*, pages 770–778, 2016.

P Kingma Diederik. Adam: A method for stochastic optimization. (*No Title*), 2014.

Reza Shokri, Marco Stronati, Congzheng Song, and Vitaly Shmatikov. Membership inference attacks against machine learning models. In *2017 IEEE symposium on security and privacy (SP)*, pages 3–18. IEEE, 2017.

Ziming Hong, Runnan Chen, Zengmao Wang, Bo Han, Bo Du, and Tongliang Liu. When data-free knowledge distillation meets non-transferable teacher: Escaping out-of-distribution trap is all you need. *arXiv preprint arXiv:2507.04119*, 2025.

Appendix

A Algorithm of proposed MeGU

In Section 4, we propose MeGU as our unlearning method. MeGU employs zero-shot MLLM as machine experts to estimate the feature similarities between different concepts, represented by a transition matrix \mathbf{T} . This matrix is subsequently used to assign perturbing labels to the dataset, instructing the utilization of feature noises to disentangle the influence of the target concept. This approach ensures effective unlearning while preserving overall generalization. To better understand the workflow of perturbing label generation, we provide a detailed pseudo-code below.

Algorithm 2 Transition matrix and perturbing labels.

Require: Instance x_i of class k from subset \mathcal{D}_{ex} selected from training set \mathcal{D} , concepts $\mathcal{Y} = \{0, 1, \dots, K-1\}$, MLLM q_w .

- 1: Let $q_w(x, y)$ represent the prompted MLLM output of image x and concept y .
- 2: **for** $k \in \mathcal{Y}$ **do**
- 3: **for** $l \in \mathcal{Y}$ **do**
- 4: $\tilde{\mathcal{S}}_{kl} = \frac{1}{n} \sum_i^n [q_w(x_i, l)], (x_i, k) \in \mathcal{D}_{ex}$ ▷ Eq. 5
- 5: **end for**
- 6: $\mathbf{t}_k = (\tilde{\mathcal{S}}_{k0}, \tilde{\mathcal{S}}_{k1}, \dots, \tilde{\mathcal{S}}_{K-1})^T / \sum_i^{K-1} \tilde{\mathcal{S}}_{ki}$
- 7: **end for**
- 8: $\mathbf{T} = (\mathbf{t}_0, \mathbf{t}_1, \dots, \mathbf{t}_{K-1})$

Require: Instance (x_i, y_i) from forget set \mathcal{D}_f , transition matrix \mathbf{T} , class concepts $\mathcal{Y} = \{0, 1, \dots, K-1\}$, pretrained model p_θ , identity matrix \mathbf{I} of size $[K, K]$, constant τ .

- 9: Let $\phi(\cdot, \tau)$ denotes the process of selecting the index of the $\lfloor K\tau \rfloor$ -th largest element.
- 10: **for** $(x_i, y_i) \in \mathcal{D}_f$ **do**
- 11: $\tilde{\mathbf{I}}_{y_i} \leftarrow \mathbf{I}[j, y_i] = 0, j \in [0, K-1]$
- 12: $\mathbf{R}_i = \mathbf{T} \cdot [\tilde{\mathbf{I}}_{y_i} \cdot p_\theta(x_i)]$ ▷ Eq. 7
- 13: $y_i^p = \phi(\mathbf{R}_i, \tau)$
- 14: **end for**

B Parameter settings for experiments

During the unlearning process, different configurations are employed for the ResNet18 and Vision Transformer (ViT) backbones to reach a balance between effectiveness and efficiency. These settings are detailed in Table 5. The "noise size" refers to the batch size of feature noise samples extracted per class, which are randomly selected to be integrated with the target data. We at one time train a batch of feature noise for one class to enrich the variety. However, empirical results show that this will not affect the overall effectiveness of our method. Thus, the noise batch size can be decreased to save computation and time costs.

Table 5: Parameter setting for unlearning.

Parameters	ResNet18	ViT
exemplar n /class	10	10
batch size	32	32
noise size	256	64
noise lr	0.1	0.1
unlearn lr	0.0003	0.00005
rank τ	0.3	0.3
proportion α	0.7	0.7
number of instances for finetune	10000	10000
finetune iteration	3	5

C Distribution of perturbing labels

In Section 4.1, we present a perturbing label assignment strategy grounded in the feature similarities between each instance in the forget set \mathcal{D}_f and the retained concepts. This strategy leverages the conceptual relationships encoded within the transition matrix \mathbf{T} , in conjunction with the predictions of \mathcal{D}_f obtained from the unlearned model, to effectively quantify such feature-level affinities.

In contrast to unbalanced label assignment methods, which often mislead the model by systematically misclassifying target instances into a single erroneous class, our approach introduces diversity in the assignment of perturbing labels across instances. This variation mitigates the risk of inducing model bias and the Streisand effect during fine-tuning, by promoting a balanced and context-aware distribution of perturbing labels. Moreover, compared with complete random label assignment, our approach systematically considers the semantic compatibility between target instances and their assigned perturbing concepts. This compatibility is quantified through feature similarity, thereby guiding the reassignment process in a principled manner. Such alignment facilitates more effective unlearning, as target instances are more likely to be aligned with semantically related concepts, reducing unintended model disruption.

Figure 5 visualizes the distribution of perturbing labels assigned to the forget dataset. This experiment is conducted on CIFAR-10, with class 2 designated as the target class, using ResNet18 as the backbone. While the observed disparities in perturbing label frequencies may partially reflect varying conceptual proximities to the target class, the overall distribution remains notably balanced, thereby validating the efficacy of our proposed assignment mechanism.

D Comparison on visualized model prediction behavior after unlearning

The alignment of the unlearned model with the "gold model" is one of the most significant indicators when evaluating the unlearning performance, as is demonstrated in Section 5.1. In order to perceptually compare our proposed method with baselines, we utilize t-SNE to visualize the predictions of the unlearned model using different methods on CIFAR-10 test set. The results are shown in Figure 6.

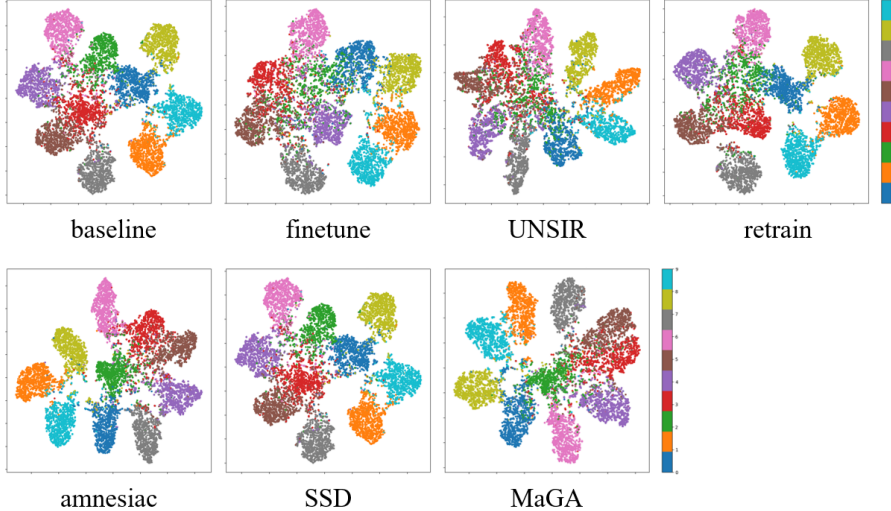


Figure 6: Visulized model prediction behavior comparison.

Each point in the figure represents an instance, while each color denotes a label (concept). Theoretically, for a model with better classification performance, the distributions of different concepts are better separated while that of the same concept should be more compact [Hong et al. \[2025\]](#). However, in class-wise unlearning scenarios, we expect model generalization on the target class to be disrupted while preserving that on retained classes. Thereby, the distribution of unlearned concept, which is designated to be label 2 represented as green, is expected to be dispersed compared with the original pretrained model (denoted as "baseline"). At the same time, the distributions of retain data are expected to maintain to preserve overall generalization. Comparing the prediction distributions of unlearned models, MeGU

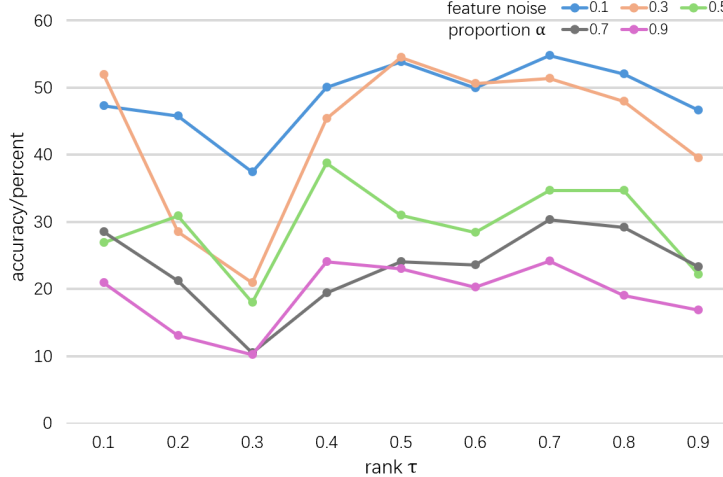


Figure 7: Performance on forget set under varying hyperparameters.

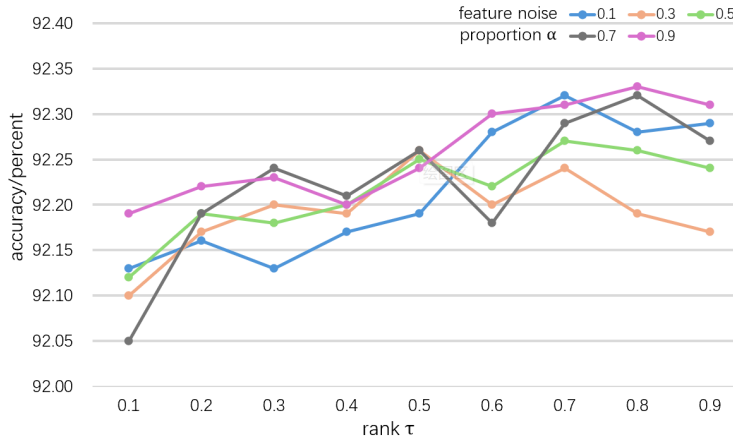


Figure 8: Performance on retain set under varying hyperparameters.

behaves more similar to the "gold model", with target instances split and captured by other well-separated retained concepts. This demonstrates the superiority of MeGU considering the closeness to the fully-retrained model.

E Sensitivity studies

In our proposed method MeGU, two key hyperparameters, the rank constant τ and the noise proportion α , play pivotal roles in the unlearning process. The rank constant τ regulates the feature similarity between the assigned perturbing labels and the corresponding target data. This is crucial, as an excessively high similarity between the reassigned and original concepts would result in the preservation of too many associated feature patterns, hindering adequate unlearning. Meanwhile, it is highlighted that the noise proportion α determines the balance between the positive feature noise encoded from the retaining data and the negative feature noise encoded from the forgetting data. As discussed in Section ??, this pair of feature noises poses different impacts on the influence disentanglement of target data during fine-tuning.

Here, to fully explore MeGU, we conduct sensitivity studies on these two hyperparameters. We record the class-wise performance of the unlearned model under varying settings using CIFAR-100 dataset. To more explicitly demonstrate the influence of different hyper-parameters on retain accuracy, we manually induce incomplete unlearning by setting the learning rate to 1e-5, which is much lower than our other experiments. We conduct 3 independent experiments for each hyperparameter setting. The averaged accuracy performance is calculated to reflect the general trend. Figure 7 and Figure 8 illustrate the classification accuracy on forget and retain dataset. It is shown that generally, a higher α represents lower accuracy in the retain set, enhancing the effects of positive feature noise on aligning perturbed instances with retain data. At the same time, the trend of retain accuracy under a changing rank τ is investigated. The

Table 6: Ablation studies on class-wise unlearning with CIFAR-100.

model	class	Metric	baseline	retrain	SSD	RND	w.o.F.N	MeGU
RN18	rocket	A_r	76.30	76.19	75.86	76.24	75.46	75.75
		A_f	82.81	0.00	0.00	56.51	3.32	0.00
		MIA	96.61	8.06	0.66	20.4	0.00	0.00
	MR	A_r	76.38	76.16	76.20	75.98	76.07	76.25
		A_f	82.03	0.00	0.00	57.12	4.55	0.00
		MIA	95.65	5.61	0.25	10.21	0.00	0.00
ViT	rocket	A_r	92.27	91.84	91.39	92.37	91.96	92.34
		A_f	93.14	0.00	0.00	56.51	3.84	0.00
		MIA	84.88	6.29	6.62	2.8	0.00	0.00
	MR	A_r	92.20	92.18	91.78	92.07	91.79	92.33
		A_f	98.44	0.00	0.00	72.66	10.17	0.00
		MIA	90.24	0.86	1.45	1.4	0.00	0.00

prior hypothesis is verified that although we intuitively expect a more similar concept as the perturbing label, such a perturbing label with too many associated feature patterns will hinder the forgetting of target information. On the other hand, there is hardly clear regularity corresponding to α or τ due to the saturated classification performance on retain data. Thus, in experiments, a τ around 0.2 to 0.3 and an α around 0.7 to 0.9 are preferred.

F Ablation studies

To deepen the understanding of the intrinsic properties of the MeGU framework and evaluate the impact of its key components: machine-guided perturbing labels and the following pair of feature noises. We conduct ablation studies using various combinations of these elements on class-wise unlearning tasks with CIFAR-100. The results are presented in Table 6, where 'RND' refers to assigning random labels to forget data instead of leveraging calculations of associated features, and 'w.o.F.N' represents fine-tuning exclusively with perturbing labels, omitting feature noises.

Compared with RND, the collaboration of MLLM guidance evidently facilitates the complete forgetting of target data, with over 50% reduction of retain accuracy and 20% decreased MIA on class rocket. It is attributed to the fine realignment effect of perturbing labels, which prevents the connections between retained feature patterns and target concepts. Without the MLLM guidance, the Fragment-Align strategy would not have functioned correctly, leading the model towards possibly the wrong tuning direction. Meanwhile, it is demonstrated that the addition of feature noises, including a pair of positive and negative feature noise, effectively disentangles and manipulates the generalization of the forget data. This guarantees a balance between complete unlearning of forgotten data and preservation of model generalization on retained data. For unlearning on class mushroom using ViT, feature noises help increase the retain accuracy by 0.54% while reducing forget accuracy by 10.17%.

Table 7: Additional results of class-wise unlearning on CIFAR-100.

model	class	metric	baseline	retrain	FT	UNSLR	AMNC	SSD	MeGU
RN18	baby	A_r	76.54	75.71	64.64	71.86	73.53	76.64	76.70
		A_f	67.80	0.00	0.00	0.00	0.00	0.00	0.00
		MIA	96.27	3.44	19.30	18.46	54.81	0.00	0.00
	lamp	A_r	76.50	75.33	64.74	71.64	73.32	76.46	76.11
		A_f	69.10	0.00	0.00	0.00	0.00	0.00	0.00
		MIA	96.20	0.63	10.74	8.68	51.89	0.00	0.00
	sea	A_r	76.35	73.16	64.00	71.14	73.45	75.11	73.36
		A_f	83.68	0.00	0.00	0.00	0.00	0.00	0.00
		MIA	9.42	4.85	34.41	36.67	27.66	1.60	1.20
	DINO	A_r	76.39	74.79	63.54	71.63	73.43	76.39	76.55
		A_f	78.13	0.00	0.00	0.00	0.00	0.00	0.00
		MIA	98.20	0.00	12.24	5.87	36.86	0.00	0.00
	wolf	A_r	76.38	76.28	63.45	71.75	72.64	76.26	76.30
		A_f	79.51	0.00	0.00	0.00	0.00	0.00	0.00
		MIA	97.40	0.49	13.62	13.84	43.45	0.00	0.00

Table 8: Additional results of sub-class unlearning on CIFAR-20.

model	subclass	metric	baseline	retrain	FT	UNSIR	AMNC	SSD	MeGU
RN18	beetle	A_r	82.63	82.35	73.23	82.00	82.20	80.10	82.37
		A_f	82.64	67.71	72.05	76.13	40.97	0.78	70.40
		MIA	88.43	20.26	58.64	71.00	9.40	8.81	6.26
	snail	A_r	83.00	81.97	75.49	80.98	82.80	82.77	83.10
		A_f	69.88	37.59	16.32	55.30	9.90	6.68	50.27
		MIA	84.50	9.47	16.57	47.22	10.05	4.80	4.33
	whale	A_r	82.90	82.09	74.81	81.66	82.08	82.67	82.74
		A_f	77.08	67.27	61.37	79.08	20.92	72.57	72.55
		MIA	85.86	36.47	54.39	77.80	3.87	61.42	26.71
	fox	A_r	82.96	82.40	71.50	82.06	81.98	79.90	82.32
		A_f	72.40	6.08	17.71	56.68	4.34	0.00	13.12
		MIA	82.46	5.60	15.66	35.43	14.61	21.80	3.70
	SCP	A_r	82.80	82.08	74.00	81.39	82.35	81.62	82.29
		A_f	90.36	67.53	61.02	82.12	5.12	7.46	69.14
		MIA	91.49	16.20	33.00	56.02	4.28	5.45	3.94

G Supplementary experiments

In Section 5, we demonstrate the effectiveness of MeGU in unlearning through a series of experiments, encompassing both class-wise and sub-class unlearning tasks on CIFAR-100 and CIFAR-20 datasets. To provide a more comprehensive evaluation of its performance, we extend the unlearning implementation to a larger number of classes (sub-classes).

Additional results of class-wise unlearning Table 7 presents results of unlearning across five different classes, where *DINO* denotes *dinosaur*. Compared to existing methods, MeGU-unlearned models exhibit a competitive alignment effect towards the retrained model. The retain accuracy of MeGU is notably maintained, showing an increase of 0.16% over SSD for the class *dinosaur*, which can be attributed to the disentanglement of retained and forgotten concepts. Additionally, it is observed that the MIA (Membership Inference Attack) risk of MeGU-unlearned models is significantly reduced. For example, the class *sea*, which presents a challenge even for the retrained model, shows a 0.4% reduction in MIA, bottoming 1.20% with MeGU, which is substantially lower than that of the retrained model. This further validates the security of the unlearning method proposed in our work.

Additional results of sub-class unlearning Table 8 presents the results of sub-classes as unlearning targets, where *SCP* denotes *skyscraper*. While certain sub-classes, such as *whale* and *skyscraper*, present more challenges in the unlearning process, MeGU still outperforms existing methods by maintaining a high alignment with the accuracy of the retrained models. For sub-classes *beetle*, *snail*, *whale*, and *skyscraper*, MeGU sticks closely to the retrained models in terms of forgetting accuracy. Additionally, it significantly reduces MIA risks across all conditions. These results further demonstrate the effectiveness of our proposed method in sub-class unlearning tasks.